

Parameter governing the far-field features of round jets

Xi Xia^{1,*} and Kamran Mohseni^{1,2,†}

¹*Department of Mechanical and Aerospace Engineering, University of Florida, Gainesville, Florida 32611, USA*

²*Department of Electrical and Computer Engineering, University of Florida, Gainesville, Florida 32611, USA*

(Received 6 May 2016; published 10 October 2016)

This study is inspired by the observation and hypothesis that the spreading and decay behaviors of a jet directly depend on the momentum-mixing mechanism between the jet and surrounding fluid. This mixing behavior is dictated by the kinematic viscosity ν for a laminar jet, which can be dramatically enhanced in a turbulent flow and is represented by the eddy viscosity ε . Similarly, pulsation in a synthetic jet is identified as another mechanism for enhancing mixing, which can be captured by an enhanced eddy viscosity beyond what is observed in a corresponding turbulent continuous jet. To this end, an effective-eddy-viscosity concept is proposed to model any excitation of a jet that could result in enhanced mixing beyond what is predicted by the kinematic viscosity. Our previous study found that ε is actuator dependent and its relationship with the spreading or decay behavior of a jet is not obvious. To remove the actuator dependence, this study performs a dimensional analysis to relate the spreading and decay behaviors to a scaled effective eddy viscosity ε/\sqrt{K} (K is the momentum flux). This quantity physically represents a competition between the radial diffusion and the axial convection of the jet axial momentum. The experimental results confirm that ε/\sqrt{K} governs the spreading and decay rates of the far field for any round jets.

DOI: [10.1103/PhysRevFluids.1.062401](https://doi.org/10.1103/PhysRevFluids.1.062401)

Round jets have been extensively studied due to their wide usages in applications as well as their fundamental significance in modeling basic shear and turbulent flows. The first theoretical benchmark for modeling a round jet is Schlichting's laminar jet solution [1]. By assuming the entire jet to be issued from a virtual but continuous point source of momentum and applying the boundary-layer approximation to the shear layer, Schlichting managed to derive a similarity solution for an incompressible axisymmetric jet issuing into a static environment. To capture the enhanced mixing of a turbulent jet, Schlichting [2] further formulated the self-similar solution for a turbulent jet by simply replacing the laminar viscosity in the boundary-layer equations with an effective eddy viscosity that is associated with the turbulent jet. The result matches well with the self-similar velocity profiles in the far field of round turbulent jets that were obtained experimentally [3–9]. Along with self-similarity, researchers [3–9] also investigated the axial variations of the jet width b and the centerline velocity u_c . Interestingly enough, they found similar behaviors in the far field of round turbulent jets, e.g., the spreading rate and nondimensional decay rate were identified to be around 0.1 and 6, respectively. The spreading and decay behaviors were also analytically studied by other researchers [10–13] and similar scaling relations ($u_c \sim x^{-1}$ and $b \sim x$) were concluded.

Different from the continuous jets introduced above, synthetic jets [14,15] are generated by periodically inhaling ambient fluid and then ejecting vortex rings [14,16]. Recently, synthetic jets have been applied in various applications [15,17–22] due to their enhanced entrainment and mixing properties [14,23–25] compared to continuous jets. Researchers have found that although fundamental differences exist in the near field, the far field of a synthetic jet displays a self-similar feature [14,24,26] that resembles a continuous turbulent jet. Based on this observation and the

*xiaxiss@ufl.edu

†mohseni@ufl.edu

XI XIA AND KAMRAN MOHSENI

TABLE I. Test matrix for five continuous jets (CJ) and three sample synthetic jets (SJ). A total of 50 synthetic jets was tested and the parameters were reported in Ref. [27]. Here d is the orifice diameter, \dot{V} is the volumetric flow rate, f is the driving frequency, and L/d is the stroke ratio. The Reynolds number is defined as $Re_s = U_s d / \nu$, where U_s is the effective jet velocity estimated at the jet exit.

Case	d (mm)	\dot{V} (L/min)	f (Hz)	L/d	Re_s
CJ1	1.0	6.0			8488
CJ2	1.0	8.0			11318
CJ3	1.0	10.0			14147
CJ4	1.5	14.0			12739
CJ5	1.5	18.0			16977
SJ9	1.0		1850	48.6	8476
SJ17	1.5		1850	14.8	5814
SJ33	2.0		1850	4.7	3284

approach Schlichting had taken to extend the Schlichting jet solution from laminar flow to turbulent flow, Krishnan and Mohseni [26] performed a similar adaptation in their synthetic-jet model by replacing the laminar viscosity with an effective eddy viscosity ε that includes the pulsatile effects of the synthetic jet.

In this study we move a step forward to show that the Schlichting jet adaptation not only satisfies self-similarity, but also provides a unified approach to model the spreading and decay behaviors for both continuous and synthetic jets. This is based on the eddy viscosity approximation that ε dictates the momentum-mixing mechanism of a jet. Krishnan and Mohseni [26] showed that ε for a synthetic jet is significantly higher than that for a continuous turbulent jet with the same jet-exit dimension and momentum flux. However, they also found that ε for a synthetic jet varies dramatically depending on the actuator configuration and driving parameters. To close the gap between the actuator dependence of ε and its apparent unified effect on jet mixing, we employ a dimensional analysis in the current study to connect the spreading rate and nondimensional decay rate to a *scaled* effective eddy viscosity (ε/\sqrt{K} , where K is the momentum flux) for any jet that has established self-similarity. This gives us a single parameter ε/\sqrt{K} that controls the spreading and decay behaviors of any round jet. Furthermore, applying the Schlichting jet solution, we show that the scaling laws take linear forms with analytically determined slopes.

In this experiment, turbulent continuous jets were created by regulating compressed air through different jet orifices at constant flow rates. Here, two different continuous jet nozzles were designed with orifice diameters d of 1.0 and 1.5 mm. The synthetic jets were created using actuators, which contain a round piezoelectric disk sealed between two aluminum parts so they form a cavity with an orifice on one side and a flexible diaphragm on the other. The synthetic-jet actuators have the same cavity dimension, which is 27.8 mm in diameter and 2.0 mm in depth, but different orifices, the diameters of which are 1.0, 1.5, and 2.0 mm, respectively. The frequency and strength of the synthetic jets were controlled by adjusting the frequency and voltage of the sinusoidal signal applied across the piezoelectric disks. The strength of a synthetic jet is characterized by the stroke length L . With the assumptions that the flow is incompressible and the shape of the diaphragm can be approximated by the static deflection of a circular membrane clamped on the edge and subject to a uniform load, L can be estimated by measuring the deflection of the piezoelectric diaphragm with a laser sensor (see Ref. [26] for details). The test parameters for continuous and synthetic jets are presented in Table I. The time-averaged velocity field of a jet was measured using a constant-temperature hot-wire anemometry system, the details of which have been reported in our previous study [27]. Since the near field of a synthetic jet (within $10d$ – $15d$ away from the jet exit) is dominated by strong vortices, flow reversal could exist and impair the accuracy of the hot wire. Therefore, this study avoided measuring the near-field region of synthetic jets.

PARAMETER GOVERNING THE FAR-FIELD FEATURES OF ...

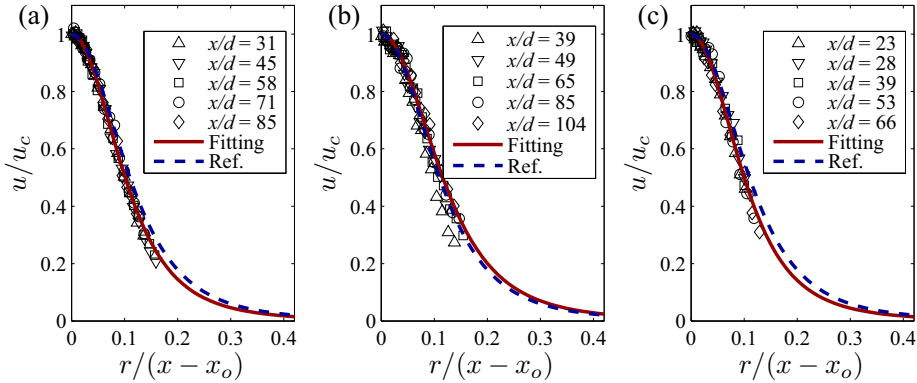


FIG. 1. Normalized velocity profiles at selected axial locations for (a) CJ5, (b) SJ9, and (c) SJ33. The axial velocity u is scaled by the centerline velocity u_c , while the radial location r is normalized by an effective axial location $x - x_o$ based on the jet's virtual origin [26,27] x_o . For comparison, the spreading rate of a reference continuous jet is fixed at 0.11.

The modeling strategy for synthetic jets in this study is inspired by the following observations and hypothesis. The spreading and decay of a jet directly depends on the momentum-mixing mechanisms between the jet and ambient fluid. Without external excitation, this mixing behavior is dictated by the physical kinematic viscosity ν . Schlichting [1] has offered an analytical solution for the spreading of a laminar jet in axisymmetric [or two-dimensional (2D)] flows. Schlichting later argued that the recognition of the importance of enhanced mixing in a turbulent flow, represented and modeled by the eddy viscosity ε , allowed this analytical solution to be extended to the case of a turbulent continuous jet [2]. We argue that in a synthetic jet there is another mode of excitation, related to the pulsed nature of the jet, that causes yet another mechanism for enhanced mixing beyond the kinematic viscosity and turbulent mixing. Following the same idea, we hypothesize that any axisymmetric (or 2D) excitation of a jet that could result in enhanced mixing beyond what is dictated by the kinematic viscosity can be represented, modeled, and measured by an effective-eddy-viscosity concept. Consequently, the analytical solution for continuous jets [2] can be extended to such cases. The adaptation of the Schlichting jet solution for round or 2D synthetic jets is supported by the match of the self-similar velocity profiles between theory and experiment, as has been demonstrated in our previous studies [26–28]. Here, Fig. 1 again shows the self-similarity for one continuous jet (CJ5) and two synthetic jets (SJ9 and SJ33).

In this study we will offer further justification of this modeling approach, in addition to the self-similarity, in terms of the relationship between spreading and decay rates for both continuous and synthetic jets. The spreading rate S_b is defined by $b_{1/2} = S_b x$, where $b_{1/2}$ is the jet half-width and the decay rate S_u is defined by $u_c = (S_u x)^{-1}$, where u_c is the centerline velocity. To better compare the decay behaviors we propose a velocity scale U_K , which is defined for each individual jet as $U_K = \sqrt{4K/\pi d^2}$, where K is the far-field momentum flux. Figures 2(a) and 3(a) plot the axial variations of the jet half-width and the inverted centerline velocity for five sample cases (CJ1, CJ5, SJ9, SJ17, and SJ33). For synthetic jets, it can be observed that the jet spreading and decay are enhanced in the axial region around $20d$; however, this enhancement gradually declines and then saturates at a downstream location ($\sim 50d$ for SJ9, $\sim 40d$ for SJ17, and $\sim 30d$ for SJ33), where the actual far field begins. This observation can be quantitatively verified in Figs. 2(b) and 3(b). Previous studies [24,26,29,30] have reported the far field of synthetic jets to start from an axial distance of $10d$ – $15d$, where the flow begins to display self-similarity. According to this study, we believe that the synthetic jet region immediately after $10d$ – $15d$, which corresponds to enhanced and varying spreading and decay rates, should be identified as an extended transitional region. Based on this

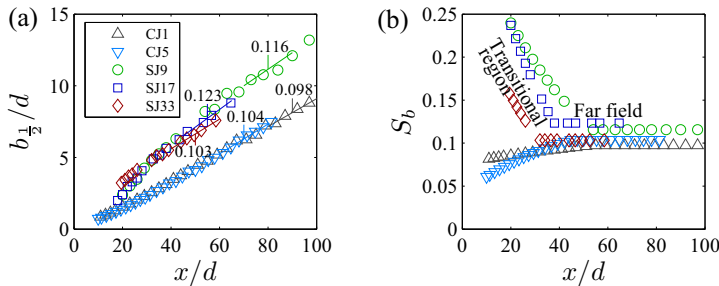


FIG. 2. (a) Axial variations of the jet half-width $b_{1/2}$ for continuous and synthetic jets. The short lines show the linear fittings of the far-field data, the slopes of which correspond to the spreading rates (CJ1, 0.098; CJ2, 0.104; SJ9, 0.116; SJ17, 0.123; and SJ33, 0.103). (b) Axial variations of the jet spreading rate S_b .

finding, the actual far field starts from $x = 30d-50d$ for different synthetic jets (see Ref. [31] for a detailed discussion).

It is worth mentioning that the spreading and decay behaviors are qualitatively similar for each jet, comparing Figs. 2 and 3. This observation clearly indicates that the spreading and decay behaviors of both synthetic and continuous jets are coupled, which will be discussed later. It is also interesting to contrast the characteristics of continuous jets with those of synthetic jets. As shown in Figs. 2 and 3, the spreading and decay rates for continuous jets increase inside the transitional region ($20d-50d$), while they decrease for synthetic jets. In particular, Figs. 2(b) and 3(b) imply that the change of spreading and decay rates in the transitional region is more gradual for continuous jets than that for synthetic jets. Although further investigation is needed, we hypothesize that the slow increase of spreading and decay rates for continuous jets might correspond to a natural (free of forcing) transition of instability and mixing from less turbulent flow to more turbulent flow; however, the intensified spreading and decay behaviors of synthetic jets within the transitional region might be caused by the strong effect of pulsation and vortex interaction, which degrades into turbulent-dominated flow as the jet evolves into the far field. Finally, the spreading and decay rates in the far field of synthetic jets approach constant values that are comparable to continuous jets. In other words, the constantlike parameters in the far field (e.g., the spreading rates being around 0.1 for a typical turbulent continuous jet) among different jets suggest that the models for continuous and synthetic jets might converge to a single approach.

To explain the above observations, we start with the basic assumption for a Schlichting jet that the far field can be considered to be a fully developed flow that originates from a virtual but continuous point source of momentum in an infinite domain. Here the momentum source of the jet is measured by the kinematic momentum flux (per unit density, in the axial direction) $K = 2\pi \int_0^\infty u^2 r dr$, where r is

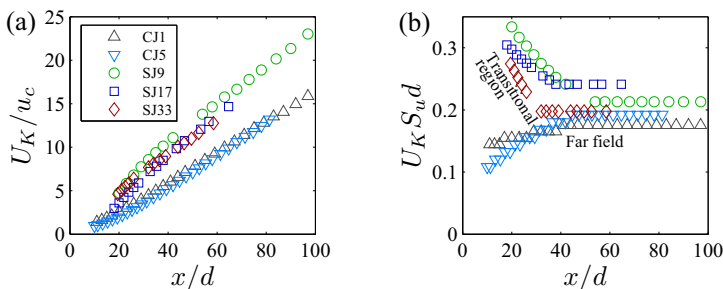


FIG. 3. (a) Axial variations of the inverted centerline velocity for the same cases shown in Fig. 2. (b) Axial variations of the nondimensional decay rate.

PARAMETER GOVERNING THE FAR-FIELD FEATURES OF ...

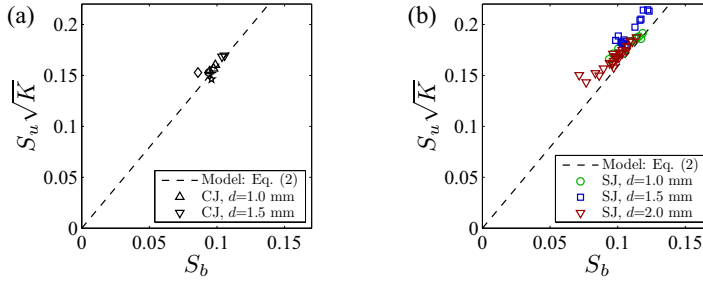


FIG. 4. Validations of $S_u\sqrt{K} = k_0S_b$ for (a) continuous jets and (b) synthetic jets. The experimental data are based on the 5 continuous jets in Table I and 50 synthetic jets reported in Ref. [27]. Continuous jets from previous studies (Ref. [4], \diamond ; Refs. [6,7], +; Ref. [8], \star ; and Ref. [9], \circ) are plotted in (a) for comparison.

the radial position and u is the axial velocity. Basically, this model requires momentum conservation in the far field, which has been validated experimentally for continuous jets that were issued into a space with sufficient spanwise dimension [6,7,9,32]. For synthetic jets, Smith and Glezer [14] found that the momentum flux decreases dramatically in the near field due to an adverse pressure gradient. Recently, Xia and Mohseni [27] added that the momentum flux decrease of a synthetic jet is directly related to the loss of impulse of the trailing jets that are formed after vortex ring pinch-off [33–35]. Nevertheless, they, together with others [23,36,37], confirmed that the momentum flux of a synthetic jet would eventually reach an asymptotic value in the far field. Therefore, we define this asymptotic value of the momentum flux as the far-field momentum flux K , an in-depth discussion of which has been provided in our previous work [27].

With the constant K assumption, the self-similar Schlichting jet solution can be obtained by solving the boundary-layer form of the Navier-Stokes equation (see Ref. [26] for details). Applying this solution, we can show that the spreading and decay rates satisfy

$$S_b = \sqrt{\frac{3K}{16\pi\varepsilon^2}}\eta_{1/2}, \quad S_u = \frac{8\pi\varepsilon}{3K}, \quad (1)$$

where $\eta_{1/2} = 2(\sqrt{2} - 1)^{1/2}$. Canceling ε in Eq. (1) yields

$$S_u\sqrt{K} = k_0S_b, \quad (2)$$

which indicates that the spreading rate is proportional to the decay rate for any round jet with the same momentum flux. Recall in Fig. 3 that $U_K S_u d$ is a nondimensional decay rate and $U_K d \propto \sqrt{K}$, so $S_u\sqrt{K} \propto S_b$ in Eq. (2) fundamentally explains the similar spreading and decay behaviors observed by comparing Figs. 2 and 3. For continuous jets, we note that although the linear relationship between S_b and $S_u\sqrt{K}$ has been reported previously [5,10–13], this model further gives the proportionality k_0 to be $[3(\sqrt{2} - 1)/\pi]^{-1/2}$.

To quantitatively validate Eq. (2), Fig. 4 plots the experimental data of $S_u\sqrt{K}$ vs S_b , which displays an overall good match with the model for both continuous and synthetic jets. For continuous jets, the results of previous studies [4,6–9] are also presented in Fig. 4(a) and show promising agreement with, in particular, the data from more recent works [6,7,9]; however, the continuous jet studied by Wagnanski and Fiedler [4] displays a small deviation from the model. This mismatch is likely to be related to the location where the momentum flux was evaluated, because the momentum fluxes in these previous studies were measured at the jet exit rather than in the far field. This would cause an overestimation of the far-field momentum flux if the momentum flux is not conserved in the axial direction. In this sense, the mismatch of Wagnanski and Fiedler actually indicates a discrepancy between the far-field momentum flux and the initial momentum flux. The momentum loss of Wagnanski and Fiedler’s jet has also been confirmed by several other studies [8,9,38], while both Capp and Hussein *et al.* attributed this momentum change to the confined spanwise dimension

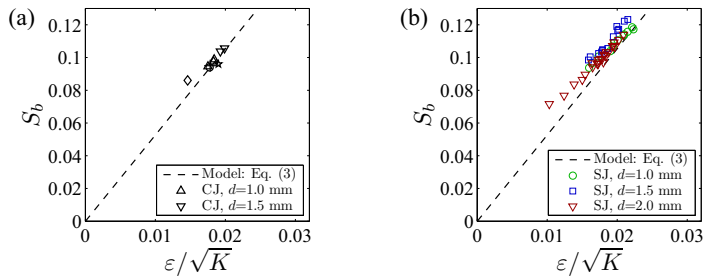


FIG. 5. Plot of S_b vs ε/\sqrt{K} for (a) continuous jets and (b) synthetic jets. All cases are the same as in Fig. 4.

of the experimental setup. In contrast, the results of Capp and Hussein *et al.* match well with the current model because their continuous jets were designed to conserve momentum flux. This suggests that Eq. (2) could serve as a criterion to evaluate momentum conservation for continuous jet experiments. For synthetic jets, some cases show a slight offset from the model. According to the above discussion, this offset could be caused by an overestimation of the far-field momentum flux. This happened because those synthetic jets become very weak in the flow field further downstream, where the hot-wire measurement encounters difficulty.

So far, we have validated this modeling approach in predicting the relationship between spreading and decay behaviors for both continuous and synthetic jets. This result provides further support for the eddy viscosity hypothesis that the momentum mixing of any jet is dictated by the effective eddy viscosity ε , which includes any mixing effects beyond the laminar and turbulent viscosity. However, Krishnan and Mohseni [26] found that ε for a synthetic jet has a strong dependence on the actuator itself (L/d and d), which seems to contradict the eddy viscosity hypothesis in that jet mixing should be a unified actuator-independent mechanism. In order to identify the true governing parameter, next a dimensional analysis is performed to relate ε to other relevant parameters. As discussed previously, ε serves as the overall mixing parameter between a jet and its ambient fluid, while the momentum flux K could be considered as a source or driving force. To this end, ε controls how laterally the momentum is transported, while K dictates the rate of axial momentum transport. Therefore, in the far field of the jet where other influences become negligible, K and ε are the only intrinsic parameters. Since the current model deals with the jet flow in a mean sense in the fully developed far field, the time t and the actuator frequency f are not included in the final formulation of this model. Nevertheless, these parameters could still affect the far field implicitly by affecting ε ; basically, f and L/d control the level of pulsation and the effective mixing represented by ε . Consequently, two parameter sets corresponding to the spreading and decay behaviors are determined to be $[K, \varepsilon, b, x]$ and $[K, \varepsilon, u_c, x]$, respectively, which result in two scaling laws after applying the Buckingham π theorem,

$$b/x = \phi_1(\varepsilon/\sqrt{K}), \quad u_c x/\sqrt{K} = \phi_2(\varepsilon/\sqrt{K}).$$

We immediately note that a *scaled* effective eddy viscosity ε/\sqrt{K} instead of ε should be the governing parameter for the jet spreading and decay behaviors. Applying the definitions of spreading and decay rates together with Eq. (1) for the Schlichting jet, the two scaling laws have the explicit forms

$$S_b = k_1 \frac{\varepsilon}{\sqrt{K}}, \quad S_u \sqrt{K} = k_2 \frac{\varepsilon}{\sqrt{K}}, \quad (3)$$

where $k_1 = [64\pi(\sqrt{2} - 1)/3]^{1/2}$ and $k_2 = 8\pi/3$. Now we use experimental data to validate the performance of Eq. (3). Since the linear relation between S_b and $S_u \sqrt{K}$ has been demonstrated in Fig. 4, we only plot S_b vs ε/\sqrt{K} for both continuous and synthetic jets in Fig. 5. Here S_b , S_u , and K are obtained directly from experimental data, while ε is estimated by $\varepsilon = S_b^2 [8(\sqrt{2} - 1)S_u]^{-1}$,

PARAMETER GOVERNING THE FAR-FIELD FEATURES OF ...

which is a by-product of the Schlichting jet solution [26]. The overall good agreement between experiment and prediction demonstrates that ε/\sqrt{K} governs the spreading and decay behaviors of both continuous and synthetic jets. Physically, ε/\sqrt{K} represents a competition between the radial diffusion and the axial convection of the axial momentum of a jet. Therefore, a larger value of ε/\sqrt{K} corresponds to stronger momentum diffusion in the radial direction, which is the result of enhanced mixing due to turbulence, pulsation, or any other type of axisymmetric excitation.

Now the behaviors of different jets can be suggested from the different values of ε/\sqrt{K} . For laminar jets, ε/\sqrt{K} is approximately 0.002 as estimated from previous studies [39,40]. From Fig. 5, ε/\sqrt{K} for all continuous turbulent jets seems to be concentrated around the value of 0.018. For synthetic jets, Fig. 5 shows that ε/\sqrt{K} for some cases grows slightly above 0.02, which is larger than continuous turbulent jets. Clearly, the larger value of ε/\sqrt{K} for those synthetic jet cases reflects the additional mixing source, analogous to the additional viscosity of turbulent jets over laminar jets. Physically, this additional mixing effect should be caused by the pulsed vortices of a synthetic jet, which is even more profound in the transitional region. Since $\varepsilon/\sqrt{K} \propto S_b$, this pulsation mechanism also explains why the spreading and decay rates are notably enhanced in the transitional region over that in the far field, as shown in Figs. 2 and 3. Therefore, we conclude that the pulsation effect of the vortices significantly enhances the effective eddy viscosity in the transitional region of a synthetic jet, while the enhancement is less pronounced in the far field where the flow is primarily dominated by the turbulent effect.

To summarize, experimental studies have shown that all continuous turbulent jets display similar spreading and mixing features [4,6–9], which are significantly enhanced over laminar jets. Schlichting [2] accounted for the enhanced spreading of turbulent jets by adding a turbulent eddy viscosity to the laminar viscosity to form an effective eddy viscosity. More recent works have demonstrated even stronger spreading and mixing features in synthetic jets [23–25]. Similar to Schlichting, here we attributed the stronger mixing of synthetic jets to the combined effect of pulsation and vortex roll-up and proposed to further add this contribution to the effective eddy viscosity. Here we note that the effective eddy viscosity is fundamentally related to the natural or forced (e.g., pulsation) instability of shear layers and the resulting vortices. Depending on the stroke ratio, a synthetic jet could display different modes of instabilities. For L/d smaller than the formation number [33], the jet flow is dominated by the forced roll-up and instability of the vortex rings. For L/d larger than the formation number, the natural instability of the trailing vortices could further increase jet mixing and spreading. This could be a topic of a future investigation. In this study, the adaptation of the Schlichting jet for both continuous and synthetic jets is further justified experimentally by the entangled relationship between spreading and decay behaviors. Through dimensional analysis, a scaled effective eddy viscosity, independent of jet actuation parameters, is identified as the governing parameter that dictates the spreading and decay rates of any jet. This finding well explains why the spreading and decay rates of some synthetic jets are higher than most continuous turbulent jets and why the spreading and decay rates of the transitional region of a synthetic jet are significantly enhanced over the far field.

This work was supported by a grant from the Office of Naval Research. We would also like to thank Dr. Adam DeVoria for providing helpful discussions and comments.

-
- [1] H. Schlichting, Laminare strahlausbreitung, *J. Appl. Math. Mech.* **13**, 260 (1933).
 - [2] H. Schlichting, *Boundary Layer Theory*, 2nd ed. (McGraw-Hill, New York, 1955).
 - [3] S. Corrsin and A. L. Kistler, The free-stream boundaries of turbulent flows, NACA TN-3133, 1954.
 - [4] I. Wignanski and H. E. Fiedler, Some measurements in the self-preserving jet, *J. Fluid Mech.* **38**, 577 (1969).
 - [5] J. O. Hinze, *Turbulence*, 2nd ed. (McGraw-Hill, New York, 1971).

- [6] S. P. Capp, Experimental investigation of the turbulent axisymmetric jet, Ph.D. thesis, SUNY Buffalo, 1983.
- [7] D. Peng, Hot wire measurements in a momentum conserving axisymmetric jet, M.Sc. thesis, SUNY Buffalo, 1985.
- [8] N. R. Panchapakesan and J. L. Lumley, Turbulence measurements in axisymmetric jets of air and helium. Part 1. Air jet, *J. Fluid Mech.* **246**, 197 (1993).
- [9] H. Hussein, S. Capp, and W. George, Velocity measurements in a high Reynolds number, momentum conserving, axisymmetric, turbulent jet, *J. Fluid Mech.* **258**, 31 (1994).
- [10] A. S. Monin and A. M. Yaglom, *Statistical Fluid Mechanics: Mechanics of Turbulence* (MIT Press, Cambridge, 1971), Vol. 1.
- [11] H. Tennekes and J. L. Lumley, *A First Course in Turbulence* (MIT Press, Cambridge, 1972).
- [12] A. A. Townsend, *The Structure of Turbulent Shear Flow*, 2nd ed. (Cambridge University Press, Cambridge, 1976).
- [13] W. K. George, in *Advances in Turbulence*, edited by W. K. George and R. Arndt (Hermisphere, New York, 1989), pp. 39–73.
- [14] B. L. Smith and A. Glezer, The formation and evolution of synthetic jets, *Phys. Fluids* **10**, 2281 (1998).
- [15] K. Mohseni and R. Mittal, *Synthetic Jets: Fundamentals and Applications* (CRC, Boca Raton, 2014).
- [16] R. Holman, Y. Utturkar, R. Mittal, B. L. Smith, and L. Cattafesta, Formation criterion for synthetic jets, *AIAA J.* **43**, 2110 (2005).
- [17] A. Seifert, S. Eliahu, D. Greenblatt, and I. Wygnanski, Use of piezoelectric actuators for airfoil separation control, *AIAA J.* **36**, 1535 (1998).
- [18] M. Amitay, D. R. Smith, V. Kibens, D. E. Parekh, and A. Glezer, Aerodynamic flow control over an unconventional airfoil using synthetic jet actuators, *AIAA J.* **39**, 361 (2001).
- [19] R. Mittal and P. Rampunggoon, On the virtual aeroshaping effect of synthetic jets, *Phys. Fluids* **14**, 1533 (2002).
- [20] M. Krieg and K. Mohseni, Thrust characterization of a bioinspired vortex ring thruster for locomotion of underwater robots, *IEEE J. Ocean. Eng.* **33**, 123 (2008).
- [21] S. Zhang and S. Zhong, Experimental investigation of flow separation control using an array of synthetic jets, *AIAA J.* **48**, 611 (2010).
- [22] L. N. Cattafesta and M. Sheplak, Actuators for active flow control, *Annu. Rev. Fluid Mech.* **43**, 247 (2011).
- [23] B. L. Smith and G. W. Swift, *Proceedings of the 15th AIAA Computational Fluid Dynamics Conference* (AIAA, Reston, 2001), paper 2001-3030.
- [24] J. E. Cater and J. Soria, The evolution of round zero-net-mass-flux jets, *J. Fluid Mech.* **472**, 167 (2002).
- [25] B. L. Smith and G. W. Swift, A comparison between synthetic jets and continuous jets, *Exp. Fluids* **34**, 467 (2003).
- [26] G. Krishnan and K. Mohseni, Axisymmetric synthetic jets: An experimental and theoretical examination, *AIAA J.* **47**, 2273 (2009).
- [27] X. Xia and K. Mohseni, Far-field momentum flux of high-frequency axisymmetric synthetic jets, *Phys. Fluids* **27**, 115101 (2015).
- [28] G. Krishnan and K. Mohseni, An experimental and analytical investigation of rectangular synthetic jets, *ASME J. Fluids Eng.* **131**, 121101 (2009).
- [29] R. Rathnasingham and K. Breuer, Coupled fluid-structural characteristics of actuators for flow control, *AIAA J.* **35**, 832 (1997).
- [30] S. G. Mallinson, G. Hong, and J. A. Reizes, *Proceedings of the 30th Fluid Dynamics Conference* (AIAA, Reston, 1999), paper 99-3651.
- [31] X. Xia and K. Mohseni, The transitional region of a round synthetic jet, *Aerosp. Sci. Technol.* (to be published).
- [32] N. E. Kotsovinos and P. B. Angelidis, The momentum flux in turbulent submerged jets, *J. Fluid Mech.* **229**, 453 (1991).
- [33] M. Gharib, E. Rambod, and K. Shariff, A universal time scale for vortex ring formation, *J. Fluid Mech.* **360**, 121 (1998).

PARAMETER GOVERNING THE FAR-FIELD FEATURES OF ...

- [34] K. Mohseni and M. Gharib, A model for universal time scale of vortex ring formation, [Phys. Fluids](#) **10**, 2436 (1998).
- [35] K. Mohseni, H. Ran, and T. Colonius, Numerical experiments on vortex ring formation, [J. Fluid Mech.](#) **430**, 267 (2001).
- [36] S. R. Fugal, B. L. Smith, and R. E. Spall, Displacement amplitude scaling of a two-dimensional synthetic jet, [Phys. Fluids](#) **17**, 045103 (2005).
- [37] J. M. Shuster and D. R. Smith, Experimental study of the formation and scaling of a round synthetic jet, [Phys. Fluids](#) **19**, 045109 (2007).
- [38] A. A. Seif, Higher order closure model for turbulent jets, Ph.D. thesis, SUNY Buffalo, 1981.
- [39] P. O'Neill, J. Soria, and D. Honnery, The stability of low Reynolds number round jets, [Exp. Fluids](#) **36**, 473 (2004).
- [40] S. J. Kwon and I. W. See, Reynolds number effects on the behavior of a non-buoyant round jet, [Exp. Fluids](#) **38**, 801 (2005).